Comparative Study of Impedance Eduction Methods, Part 1: DLR Tests and Methodology

Stefan Busse-Gerstengarbe[1], Friedrich Bake[2], Lars Enghardt[1,2]
and
Michael G. Jones[3]

[1] *Technische Universität Berlin, 10623 Berlin, Germany*

[2] *German Aerospace Center (DLR), 10623 Berlin, Germany*

[3] *NASA Langley Research Center, Hampton, VA 23681*

The absorption efficiency of acoustic liners used in aircraft engines is characterized by the acoustic impedance. World wide, many grazing flow test rigs and eduction methods are available that provide values for that impedance. However, a direct comparison and assessment of the data of the different rigs and methods is often not possible because test objects and test conditions are quite different. Only a few papers provide a direct comparison. Therefore, this paper together with a companion paper, present data measured with a reference test object under similar conditions in the DLR and NASA grazing flow test rigs. Additionally, by applying the in-house methods Liner Impedance Non-Uniform flow Solving algorithm (LINUS, DLR) and Convected Helmhholtz Equation approach (CHE, NASA) on the data sets, similarities and differences due to underlying theory are identified and discussed.

I. Introduction

During the past 40 years, there has been a world-wide emphasis on the development of grazing flow test rigs and different methods for analyzing acoustic aircraft liners. However, there are only a few direct comparisons between data of different test rigs available. One such comparison was provided by Jones,[1] which compared results acquired with four flow rigs in the United States, as well as with corresponding normal incidence tubes. For those tests, two sets of Helmholtz resonator liners with different porosity, hole diameter and sheet thickness were used. The conclusion drawn in the paper is basically the fact that all techniques more or less agree with each other. The main deviations are found for the different grazing flow assumptions, whereas similar flow approaches (e.g. plug flow) compare favorably.

This comprehensive study provided a fundamental overview of the test rigs and methods. Meanwhile, the NASA grazing incidence tube (GIT) used in the study was first highly improved[2] and finally replaced by the redesigned grazing flow impedance tube (GFIT).[3,4] In parallel the impedance eduction techniques were also improved.[5–7]

The situation and development in Europe was quite similar. There are also several rigs[8–10] and several techniques[11,12] to characterize liners for different application. In Germany, the German Aerospace Center (DLR), Engine Acoustics Department, in Berlin started work on liners together with TU Berlin. As part of this collaboration, DLR built the DUct aCoustic Test rig with Square cross section (DUCT-S) to evaluate different liners.[13–16] In addition, an analysis technique with scattering coefficients[17] and two impedance eduction methods were developed utilizing the data of the rig.[15,16,18–20] Several improvements of the DUCT-S[14] also lead to a redesigned version named DUct aCoustic Test rig with Rectangular cross section (DUCT-R) that supports liners with a length of up to 800 mm.

This made the collaborative work on a reference test object possible which is reported in the following: In the first of the two associated papers the test rig DUCT-R and the reference test object HR-S2 (Helmholtz Resonator Sample 2) - measured in both rigs, DUCT-R and GFIT - are described. The methodology of DLR is recalled and results of scattering coefficients of the tests in Berlin are shown. Additionally, impedance data of the DLR eduction technique LINUS (Liner Impedance Non-Uniform flow Solving algorithm) are compared to the NASA results. The second paper[21] deals with tests of the same reference test object at NASA in the GFIT test rig, comparing different eduction approaches and flow assumptions. The aim of the study is to compare rigs and methods with an identical test object, emphasizing the influence of both Mach number and SPL.

II. Methodology

The acoustic properties of the test object are characterized using the following approaches. These approaches have been described in detail earlier,[15,16,22] and are briefly described here for convenience.

A. Reflection, Transmission and Dissipation

A flow duct (e.g. DUCT-R) with the test object/liner located in the center is excited from upstream and downstream direction via loudspeakers. Microphones also placed up- and downstream of the liner are used to acquire acoustic pressure signals. These data are then used to calculate the amplitude ratios for reflected and transmitted waves $r^{\pm}$ and $t^{\pm}$ for both directions of propagation (upstream $(-)$ and downstream $(+)$). The acoustic energy balance for an acoustic absorber utilizing $r^{\pm}$ and $t^{\pm}$ together with the mean Mach number M to define the dissipation $\Delta^{\pm}$ then reads:[23]

$$\Delta^{\pm} = 1 - \left(\frac{(1 \mp M)^2}{(1 \pm M)^2} \cdot \left|r^{\pm}\right|^2 + \left|t^{\pm}\right|^2 \right) \tag{1}$$

Were $R = |r^{\pm}|^2$ and $T = |t^{\pm}|^2$ define the energy values of reflection and transmission.

B. Impedance Eduction Method LINUS

In the next step the 2D duct model of Mungur and Gladwell[24] is used. Then, based on the transmission coefficient $t^{\pm}$ and assuming very low reflections, the wave number for the lined part of the duct k_x is defined. For the similar NASA approach PBU-SM, axial sound pressure level $\frac{dSPL(x)}{dx}$ and phase decay $\frac{d\phi}{dx}$ are used.[3,21] The wave number k_x is then a solution of the Pridmore-Brown equation[21,25] and is defined as follows:

$$\Re\{k_x\} = \frac{d\phi}{dx} = \frac{-\arctan\left(\frac{\Im\{t\}}{\Re\{t\}}\right)}{L} \tag{2}$$

$$\Im\{k_x\} = \frac{dSPL(x)}{20\log_{10}(e)dx} = \frac{\ln(|t|)}{L} \tag{3}$$

As described in Ref. 16 this wave number is normalized with the free field wavenumber k_0. Together with local Mach number M and by integrating the pressure derivatives $\frac{dP}{dY}$ via a Runge-Kutta method along the duct height H, the complex impedance ζ is determined:

$$\zeta = \frac{Z(Y=1)}{\rho c} = -ik_0 H \left(1 - M(Y=1)\frac{k_x}{k_0}\right)^2 \cdot \frac{P(Y=1)}{\frac{dP}{dY}|_{Y=1}} \tag{4}$$

In this case the dimensionless position $Y = 1$ denotes the lined wall and $Y = 0$ the hard wall at the opposite side, where the integration algorithm starts.

III. Measurements

A. DUct aCoustic Test Rig - Rectangular cross section (DUCT-R)

Based on the measurement concept described above, which is already applied to the DUCT-S rig, the DUCT-R was designed as follows (Fig. 1): It consists of an upstream part and downstream part which are connected to the liner mounting in the middle. A radial compressor is connected to the upstream part via a tube system to provide a flow. For the cross-sectional area of 60 mm×80 mm a centerline Mach number of around 0.3 is achieved in the liner region. Both the upstream part and downstream part of the duct are divided into two microphone modules and a loudspeaker module. These modules contain an overall number of 106 microphone positions which are spread over the rig in the following order: At sixteen axial positions six microphone slots are mounted around the circumference of the duct to allow the analysis of higher order modes. Six of these rings at both sides build axial arrays which are non-equidistant but with exponentially increasing distance between the neighboring microphones. Therefore, a data analysis for a wide frequency range is possible. The arrays are placed in a manner

to suppress influences of evanescent modes in the vicinity of the loudspeakers and the near field of the liner. Nonetheless, two additional rings per side provide data of this region near the liner. During the tests, the microphone ring nearest the liner leading edge was used to adjust the target reference SPL. For the current tests, only six microphone slots of the array at both sides were equipped with G.R.A.S 40BP-S1 condenser microphones and 26AC pre-amplifiers. They were flush-mounted in the center of the side wall, because the wall pressure at one circumferential position is representative when analyzing plane wave propagation. For the same reason, only one loudspeaker (type Monacor KU-516) in each loudspeaker section was connected to the duct via a horn. These loudspeakers were fed by an Agilent arbitrary frequency generator and amplified with a KME SPA 240 E amplifier. Microphone and frequency generator signals were recorded with an OROS OR36 data acquisition system. Recording time was set to 10 s, with a sampling frequency of 8192 Hz. Additionally, temperature probes were placed upstream and downstream of the liner to allow determination of the speed of sound.
The test object was mounted on the side wall in the axial center of the duct, as shown in Fig. 1.

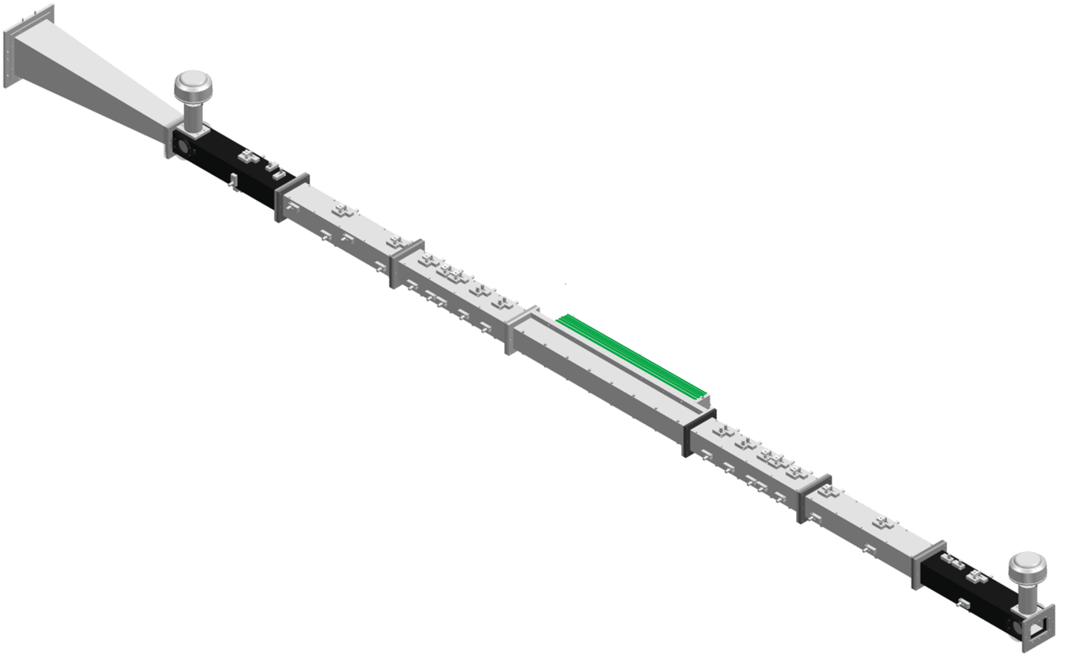

Figure 1: 3D-view of the DLR test rig DUCT-R, the test object (green) is mounted in the center as the side wall .

B. Reference Test Object: Helmholtz Resonator Sample 2 (HR-S2)

The reference test object is a generic type of Helmholtz resonator (Fig. 2) based on the design of Fischer which was already used for the similar test object HR-S1.[16] It is a single layer liner, consisting of an aluminum perforated facesheet, tubes of polycarbonate as cells and a solid back plate. The liner is designed to have its Helmholtz resonance frequency near 1 kHz, i.e. below the cut-on frequency of the DUCT-R (i.e. ≈2100 Hz) but with a quarter-wavelength resonance above cut-on. Both hole diameter and facesheet thickness are 1 mm. When manufacturing the facesheet and drilling the holes, special attention was paid to keep the rim of the holes clean and sharp-edged. The cells are 6.9 mm in diameter and 40 mm in depth. Every cell is staggered axially but aligned with the centerline of one hole to build an array of locally reacting single resonators. Due to this pattern the porosity of the facesheet is 1.5%. The whole structure is bonded together with resin and is inserted in a 558.2 mm long frame that fits in the GFIT and also as described in the DUCT-R.

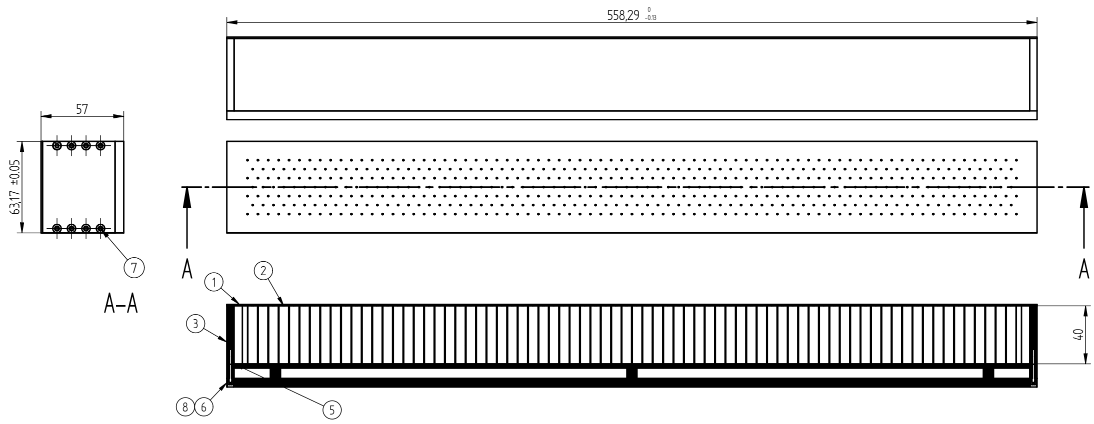

Figure 2: Reference test object HR-S2; dimensions given in mm.

C. Test Conditions DUCT-R

In a first step flow profiles were acquired to characterize the flow field and calculate boundary layer data of the test rig. In a second step acoustic tests were used applying the above mentioned methodology.

1. Flow Profile Measurements

Very similar to the tests in the NASA GFIT shown in the companion paper,[21] the sample was tested with centerline Mach numbers 0.0, 0.1, and 0.2. The mean Mach numbers which provide a good measure for comparing the two ducts had to match the conditions in GFIT. Therefore, a 3 mm Prandtl's pitot tube was traversed along the horizontal duct axis for the different centerline Mach numbers. The pressure data was acquired with a MKS Baratron connected to a data acquisition/switch unit HP 34970 A.

2. Acoustic Field Measurements

Besides the grazing flow Mach number the SPL was changed between 110, 120 and 130dB. In contrast to the GFIT tests, which used a single-tone excitation, a multi-tone excitation was used[14] for the results shown here. These multi-tones covered a frequency range between 204 and 2142 Hz. To suppress the interaction of higher harmonic tones in one signal, the frequency range was split into five signals. The peak SPL of the constituent frequencies were adjusted via the reference microphone to fit the single tone SPL measured in the GFIT.[21] Since it is mandatory for the analysis method, these tests were conducted with both upstream and downstream sources.

IV. Results

A. Flow Profiles

The flow profiles for all three Mach numbers are shown in Fig. 3. The blue circles represent the measured data while the red curve is a cubic-spline fit to interpolate in between. The software of Bauers[26] is fed with the interpolated data which calculates the boundary layer thickness δ_{99}, displacement thickness δ_1 and momentum thickness δ_2 for ether part of the profile top (t) and bottom (b) as well as the mean Mach number M. These values are given in Tab. 1 for the respective centerline Mach number. The profiles are slightly asymmetric. However, the values nearly match data of the GFIT presented by Jones[3] with a similar setup as described in the companion paper.[21]

Table 1: Boundary layer data of DUCT-R for different centerline and mean Mach numbers (M_{cl} and M) calculated from flow profiles measured upstream of the liner (Fig. 3). b-bottom part of the profile, t-top part of the profile with the liner.

M_{cl} [1]	M [1]	$\delta_{99}^b [mm]$	$\delta_{99}^t [mm]$	$\delta_1^b [mm]$	$\delta_1^t [mm]$	$\delta_2^b [mm]$	$\delta_2^t [mm]$
0.1	0.0922	21.0	31.9	3.6	5.4	2.3	3.1
0.2	0.1863	20.9	27.8	3.3	4.4	2.1	2.6

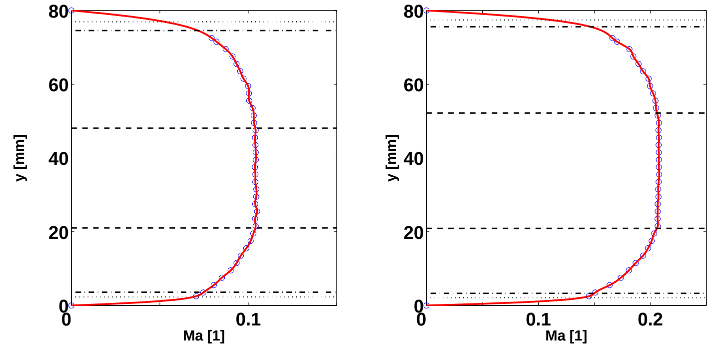

(a) $M_{cl} = 0.1/M = 0.0922$ **(b)** $M_{cl} = 0.2/M = 0.1863$

Figure 3: Flow profiles (horizontal component) of the DUCT-R measured in front of the lined section. Blue circles - measured data, red line - cubic spline fit, dashed line - boundary layer thickness δ_{99}, dot-dashed line - displacement thickness δ_1 and dotted line - momentum thickness δ_2.

B. Scattering Coefficients Calculated from DUCT-R Data

As described in Section II, scattering coefficients are calculated from the microphone pressure signals. The results in Fig. 4 show the general damping behavior of the sample. The rows show results of different Mach numbers at different peak SPL (columns).

For the no-flow case in Fig. 4a, the lowest transmission is found for the desired frequency around 850 Hz. This matches with the results of the similar HR-S1 Liner.[16] Nonetheless, in this case small reflections (<10%) are detected at resonance frequency. However, this small peak disappears for the flow cases and higher SPL and therefore allows application of the LINUS method (see Section II).

Furthermore, an increasing SPL results in a broader dissipation and transmission curve for the no-flow cases. Since both impedance data sets (DLR/NASA) also slightly change their resistance through higher SPL (see Section IV.C and Ref. 21) toward 1 ρc, such an increased dissipation should be the result.

As expected from other data,[15] a broadening of the dissipation and transmission spectra is also visible for higher Mach numbers (Fig. 4d-4g). This effect is observed for all SPL levels. When the Mach number is increased, the maximum dissipation in the upstream direction decreases (≈-25%). A similar result is observed for the downstream direction, but the maximum dissipation is more gentle (≈-10%). The observations for similar test objects were different for the last aspect, since there the downstream direction had a constant high level with a sort of saturation for increasing Mach number.[15] However, the expected frequency shift for the maximum dissipation is visible when the Mach number is increased.

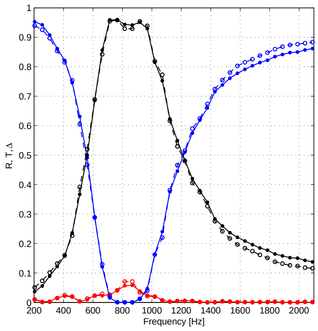

(a) SPL=110 dB, M_{cl} =0

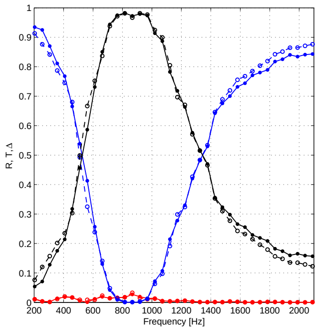

(b) SPL=120 dB, M_{cl} =0

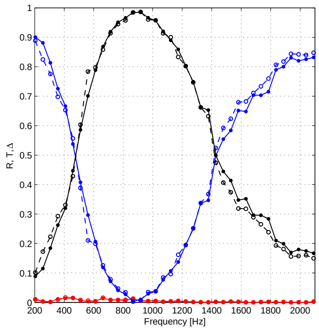

(c) SPL=130 dB, M_{cl} =0

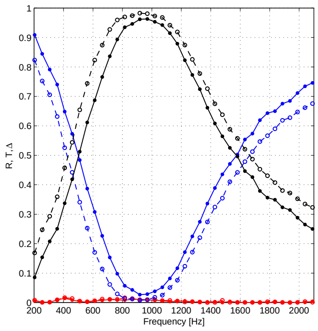

(d) SPL=110 dB, M_{cl} =0.1

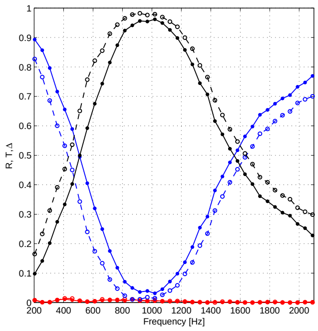

(e) SPL=120 dB, M_{cl} =0.1

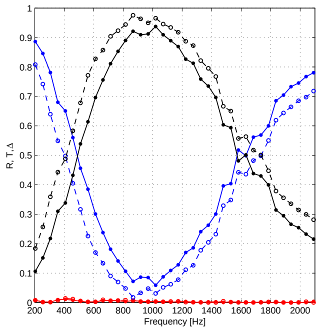

(f) SPL=130 dB, M_{cl} =0.1

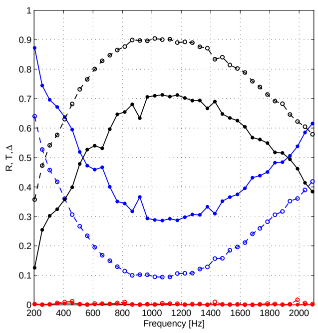

(g) SPL=110 dB, M_{cl} =0.2

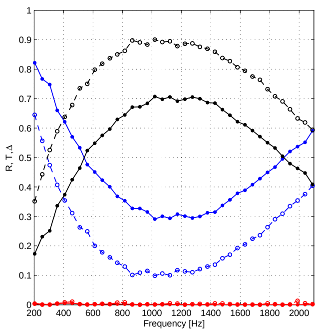

(h) SPL=120 dB, M_{cl} =0.2

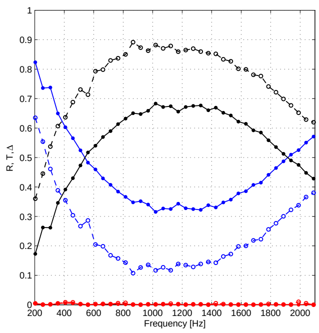

(i) SPL=130 dB, M_{cl} =0.2

Figure 4: Comparison of scattering coefficients for different Mach numbers (rows) at different peak SPL (columns). Energy reflection R - red lines, energy transmission T - blue lines and energy dissipation Δ - black lines. Solid lines for downstream direction (+) and dashed lines for upstream direction (−).

C. Comparison of Impedance Data

The transmission coefficient is then used in the described manner to educe the impedance. Figures 5, 6 and 7 show the direct comparison of GFIT data analyzed with the Convected Helmholtz Equation (CHE) approach[21] and DUCT-R data applying the LINUS method. For both methods an uniform-flow of mean Mach number M is used and only plane wave propagation is analyzed. In the figures the normalized resistance is shown with blue symbols while red symbols denote the normalized reactance.
For 110 dB excitation SPL, the reflections at the no-flow condition are too large to allow proper usage of the LINUS method for impedance eduction. Hence, only those results achieved at Mach numbers of 0.1 and 0.2 are presented (Fig. 5). For these conditions, the trends for both resistance and reactance are quite similar for frequencies up to 1400 Hz. Nonetheless, there is a divergence between the data sets for higher frequencies which has to be investigated further. However, for $M = 0.1$ both reactance curves cross the abscissa around 1150 Hz which defines the resonance frequency of the sample. When increasing the Mach number to 0.2 the slope of the reactance flattens out. This behavior is observed for both methods LINUS and CHE.[21] Furthermore, the resistance is increasing with increasing Mach number. This indicates the liner to be non-linear regarding Mach number.
The results of the second excitation level (120 dB) are shown in Figure 6. Reflections are low enough at the no-flow condition, so data can also be presented for this case. There is a very good agreement, especially for the reactance. Furthermore, the trends of the flow cases are similar to those of 110 dB excitation. Resistance increases and reactance flattens due to higher Mach number. However, the reactance slope of DUCT-R/LINUS data flattens and shifts much more for $M = 0.2$ than is observed for the GFIT/CHE data.
Finally, the data of 130 dB follows the same trends (Fig. 7). Even though DUCT-R data is not smooth, distinct "‘dropouts"’ visible for the GFIT reactance spectra are not found. Therefore, this effect due to harmonic distortion is further discussed in the companion paper.[21] Possibly, the characteristics of the drivers or the excitation in general for such high levels are different for both rigs.

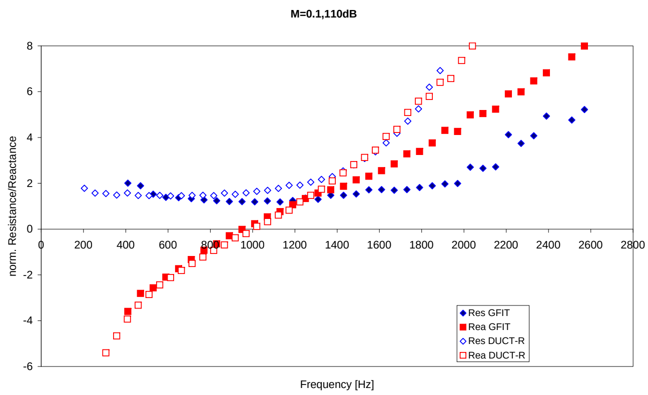

(a) SPL=110 dB, M_{cl} =0.1/$M = 0.0922$

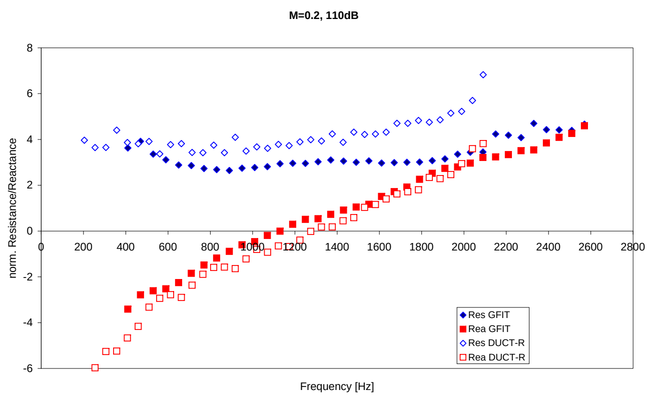

(b) SPL=110 dB, M_{cl} =0.2/$M = 0.1863$

Figure 5: Comparison of educed impedance data for $M = 0.1$ and 0.2 at 110dB. The normalized resistance is shown with blue symbols while red symbols denote the normalized reactance. Closed symbols represent NASA GFIT data and CHE eduction method,[21] open symbols represent DLR DUCT-R data and LINUS eduction method.

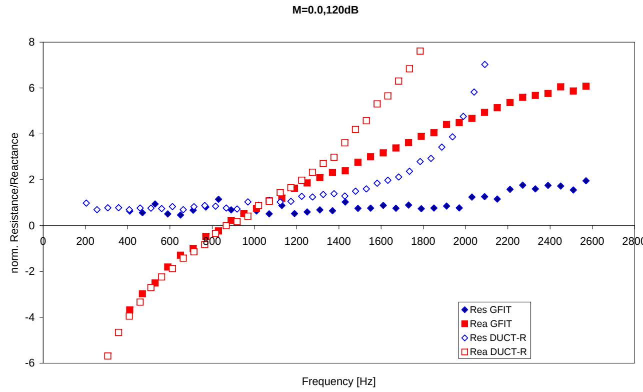

(a) SPL=120 dB, M_{cl} =0/$M = 0$

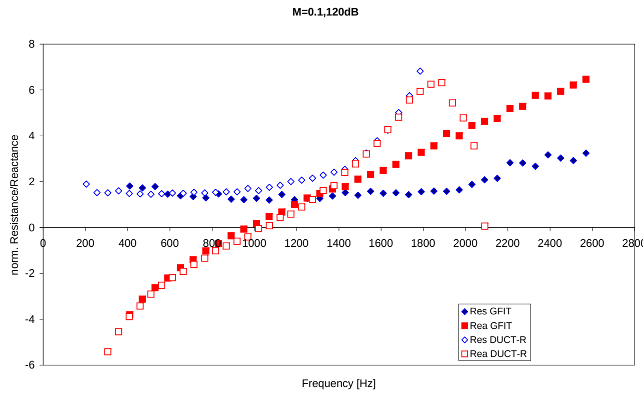

(b) SPL=120 dB, M_{cl} =0.1/$M = 0.0922$

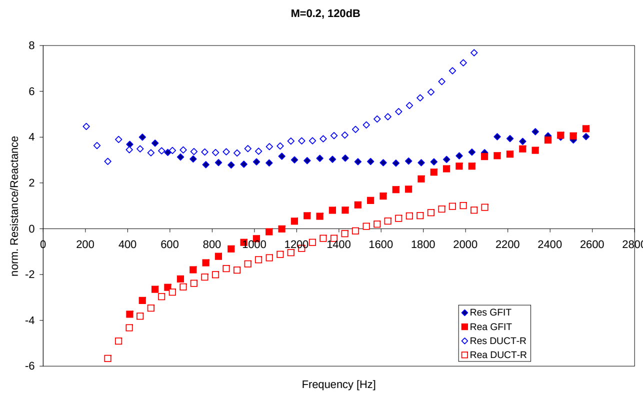

(c) SPL=120 dB, M_{cl} =0.2/$M = 0.1863$

Figure 6: Comparison of educed impedance data for for all Mach numbers at 120dB. The normalized resistance is shown with blue symbols while red symbols denote the normalized reactance. Closed symbols represent NASA GFIT data and CHE eduction method,[21] open symbols represent DLR DUCT-R data and LINUS eduction method.

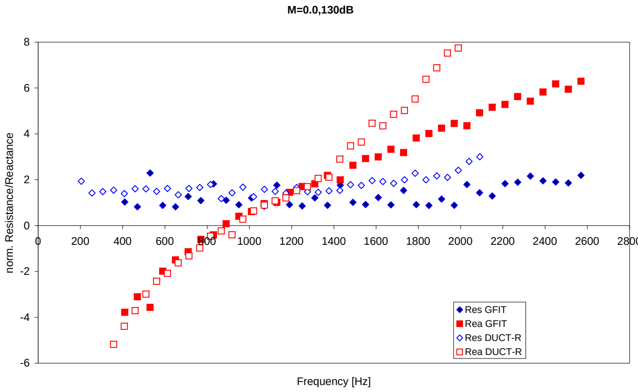

(a) SPL=130 dB, M_{cl} =0/$M = 0$

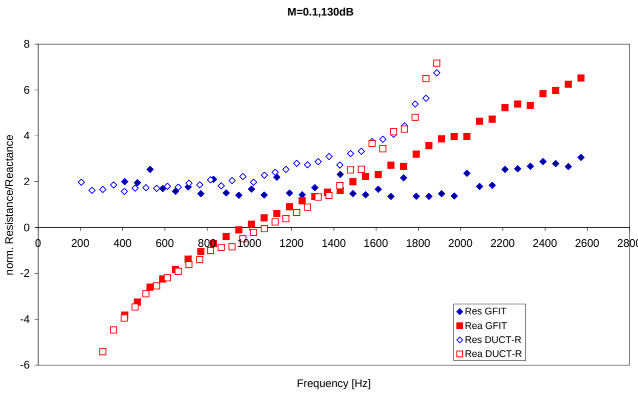

(b) SPL=130 dB, M_{cl} =0.1/$M = 0.0922$

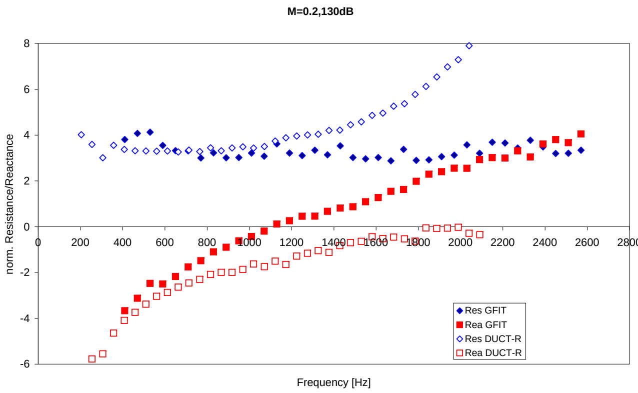

(c) SPL=130 dB, M_{cl} =0.2/$M = 0.1863$

Figure 7: Comparison of educed impedance data for all Mach numbers at 130dB. The normalized resistance is shown with blue symbols while red symbols denote the normalized reactance. Closed symbols represent NASA GFIT data and CHE eduction method,[21] open symbols represent DLR DUCT-R data and LINUS eduction method.

V. Conclusion

Similar to the survey of Jones[1] a decade ago this study provides a comparison of two different state of the art approaches to educe liner impedance. The same reference test object, a Helmholtz resonator liner, is tested in the rigs GFIT (NASA) and DUCT-R (DLR) under similar conditions. The measured microphone data was analyzed using the respective impedance eduction methods. First, an in-house code that provides scattering coefficients and wavenumber data was used to determine the impedance. In addition, the NASA approach that is based on the convected Helmholtz equation (CHE) utilizes the acoustic pressure data to find the impedance. The following conclusions can be drawn from these results.

1. The investigated reference test object is mainly a dissipative liner, i.e. the high transmission loss is provided through high dissipation while reflections are nearly negligible.
2. Furthermore, the scattering coefficients (i.e. transmission and dissipation) show a dependency on source SPL and Mach number. The spectra gently broaden for an increasing SPL while peak attenuation is nearly constant or slightly increasing.
3. A greater dependency is found for increasing Mach number. The spectra also broaden for both upstream and downstream direction but the maximum dissipation is reduced. Against expectation, this holds true for both directions of wave propagation.
4. A Mach number dependency is also observed for the educed impedances. Especially the resistance is highly influenced by this parameter. Therefore, the utilized reference test object is identified to be non-linear (concerning Mach number[21,27]). However, the Mach number influence on the reactance is only weak but visible.
5. Over the range of Mach numbers and excitation SPL used in this test, impedances educed via the LINUS and CHE methods compare favorably for frequencies at or below resonance. However, they diverge for frequencies above resonance. Further research is needed to better understand these effects.
6. In general it can be concluded that even for different measurement approaches and eduction techniques the impedance data is in the same range.

Acknowledgements

The authors grateful acknowledge the support of Andre Fischer, Wolfram Hage, Manfred Ziehe, Horst Mettchen, Thorsten Dessin, Lech Modrzejewsk, Nancy Kings, Mirko Spitalny, Tiago Werner, Steffen Nitsch, Claus Lahiri and Anita Schulz when manufacturing and testing the Liner HR-S2. Moreover, we thank Roland Bauers who provided the software for flow field data analysis which was adapted by Lisa Kosanke.
The author Stefan Busse-Gerstengarbe wish to express his sincere gratitude for the warm welcome and the support of the whole NASA team during the tests at NASA Langley Research Center.
This work was funded by the German Research Foundation (DFG) in the framework of the Project UNLIMITED (TH 288/35-1).

References

[1] Jones, M. G., Parrott, T. L., and Watson, W. R., "Comparison of acoustic impedance eduction techniques for locally-reacting liners," *9th AIAA/CEAS Aeroacoustics Conference and Exhibit*, No. AIAA 2003-3306, Hilton Head, South Carolina, May 12-14 2003, pp. 1837–1847.

[2] Jones, M., Watson, W. R., and Nark, D. M., "Optimization of Acoustic Pressure Measurements for Impedance Eduction," *13th AIAA/ CEAS Aeroacoustics Conference (28th AIAA Aeroacoustics Conference)*, No. AIAA 2007-3531, Rome, Italy, 2007.

[3] Jones, M. G., Watson, W. R., and Nark, D. M., "Effects of Flow Profile on Educed Acoustic Liner Impedance," *16th AIAA/CEAS Aeroacoustics Conference*, No. AIAA 2010-3763, Stockholm, Sweden, June 7-9 2010.

[4] Jones, M. and Watson, W., "On the Use of Experimental Methods to Improve Confidence in Educed Impedance," *17th AIAA/CEAS Aeroacoustics Conference (32nd AIAA Aeroacoustics Conference)*, No. AIAA 2011-2865, Portland, Oregon, 5-8 June 2011.

[5] Watson, W. R., Jones, M., and Parrott, T., "Investigation of an Anomaly Observed in Impedance Eduction Techniques," *14th AIAA/ CEAS Aeroacoustics Conference (29th AIAA Aeroacoustics Conference)*, No. AIAA 2008-3013, Vancouver, Canada, May 5 - 7 2008.

[6]Watson, W. and Jones, M., "Validation of a New Procedure for Impedance Eduction in Flow," *16th AIAA/CEAS Aeroacoustics Conference*, No. AIAA 2010-3764, Stockholm, Sweden, June 7-9 2010.

[7]Watson, W., Jones, M., and Gerhold, C., "Implementation and Validation of an Impedance Eduction Construction and Validation of A Broadband Time Domain Impedance Boundary Condition Technique," *17th AIAA/CEAS Aeroacoustics Conference (32nd AIAA Aeroacoustics Conference)*, No. AIAA 2011-2868, Portland, Oregon, 5-8 June 2011.

[8]Zandbergen, T., "Acoustic and Aerodynamic Characteristics of Perfolin, The Linear Perforated Plate Acoustic Liner," *11th Aeroacoustics Conference*, No. AIAA 1987-2740, Paolo Alto, California, Oct. 19 - 21 October 1987.

[9]Åbom, M., "Measurement of the scattering-matrix of acoustical two-ports," *Mechanical Systems and Signal Processing*, Vol. 5, No. 2, 1991, pp. 89 – 104.

[10]Murray, P. B., Ferrante, P., and Scofano, A., "Manufacturing Process and Boundary Layer Influences on Perforate Liner Impedance," *11th AIAA/CEAS Aeroacoustics Conference (26th AIAA Aeroacoustics Conference)*, No. AIAA 2005-2849, Monterey, California, May 23-25 2005.

[11]Elnady, T., Bodén, H., and Elhadidi, B., "Validation of an Inverse Semi-Analytical Technique to Educe Liner Impedance," *AIAA Journal*, Vol. 47, No. 12, December 2009, pp. 2836–2844.

[12]Piot, E., Primus, J., and F., S., "Liner impedance eduction technique based on velocity fields," *18th AIAA/CEAS Aeroacoustics Conference (33rd AIAA Aeroacoustics Conference)*, No. AIAA 2012-2198, Colorado Springs, USA, June 4-6 2012.

[13]Busse, S., Richter, C., Heuwinkel, C., Enghardt, L., Röhle, I., Michel, U., Thiele, F., Ferrante, P., and Scofano, A., "Impedance Deduction Based on Insertion Loss Measurements of Liners under Grazing Flow Conditions." *14th AIAA/CEAS Aeroacoustics Conference (29th AIAA Aeroacoustics Conference)*, No. AIAA 2008-3014, Vancouver, Canada, May 5-7 2008.

[14]Busse, S., Richter, C., Nitsch, S., Thiele, F., Bake, F., Enghardt, L., Kückens, C., and Müller, U., "Acoustic investigation of a specially manufactured non-locally reacting liner for aircraft application," *16th AIAA/CEAS Aeroacoustics Conference (31st AIAA Aeroacoustics Conference)*, No. AIAA 2010-3830, Stockholm, Sweden, June 7-9 2010.

[15]Busse-Gerstengarbe, S., Richter, C., Lahiri, C., Enghardt, L., Roehle, I., Thiele, F., Ferrante, P., and Scofano, A., "Impedance Eduction Based on Microphone Measurements of Liners under Grazing Flow Conditions." *AIAA Journal*, Vol. 50, No. 4, April 2012, pp. 867–879.

[16]Enghardt, L., Fischer, A., Schulz, A., and Busse-Gerstengarbe, S., "Determination of the impedance for lined ducts with grazing flow," *18th AIAA/CEAS Aeroacoustics Conference (33rd AIAA Aeroacoustics Conference)*, No. AIAA 2012-2243, Colorado Springs, USA, 4-6 June 2012.

[17]Heuwinkel, C., Enghardt, L., and Röhle, I., "Experimental Investigation of the Acoustic Damping of Perforated Liners with Bias Flow," *12th AIAA/CEAS Aeroacoustics Conference (27th AIAA Aeroacoustics Conference)*, No. AIAA 2007-3525, Rome, Italy, May 21-23 2007.

[18]Richter, C., Thiele, F., Li, X., and Zhuang, M., "Comparison of Time–Domain Impedance Boundary Conditions by Lined Duct Flows," *12th AIAA/CEAS Aeroacoustics Conference (27th AIAA Aeroacoustics Conference)*, No. AIAA 2006-2527, Cambridge, Massachusetts, May 2006.

[19]Richter, C., Hay, J. A., Panek, L., Schönwald, N., Busse, S., and Thiele, F., "A review of time-domain impedance modelling and applications," *Journal of Sound and Vibration*, Vol. 330, No. 16, 2011, pp. 3859 – 3873, special issue on Computational Aero-Acoustics (CAA) for Aircraft Noise Prediction - Part A.

[20]Bassetti, A., Guerin, S., and Busse, S., "Validation of the CAA Solver PIANO with lined-wall boundary conditions," *37. Deutsche Jahrestagung für Akustik (DAGA) 2011*, Deutsche Gesellschaft für Akustik, Düsseldorf, Germany, March 21-24 2011, pp. 289–290, ISBN: 978-3-939296-02-7.

[21]Jones, M., Watson, W., Howerton, B., and Busse-Gerstengarbe, S., "Comparative Study of Impedance Eduction Methods, Part 2: NASA Tests and Methodology," *19th AIAA/CEAS Aeroacoustics Conference (34th AIAA Aeroacoustics Conference)*, Berlin, Germany, 27-29 May 2013, (submitted for publication).

[22]Lahiri, C., Enghardt, L., Bake, F., Sadig, S., and Gerendas, M., "Establishment of a High Quality Database for the Acoustic Modeling of Perforated Liners." *Journal of Engineering for Gas Turbines and Power.*, Vol. 133, No. 9, 2011, 091503.

[23]Blokhintsev, D., "Acoustics of a Nonhomogeneous Moving Medium (1946)," Translation: NACA, Technical Memorandum 1399, NACA, 1956.

[24]Mungur, P. and Gladwell, G. M. L., "Acoustic wave propagation in a sheared fluid contained in a duct," *Journal of Sound and Vibration*, Vol. 9, No. 1, 1969, pp. 28 – 48.

[25]Pridmore-Brown, D. C., "Sound Propagation in a Fluid Flowing through an Attenuating Duct," *The Journal of the Acoustical Society of America*, Vol. 30, No. 7, 1958, pp. 393–406.

[26]Bauers, R. and Tapken, U., "Separation of hydrodynamic perturbations in acoustic liner insertion loss measurements at a fan rig," *Proceedings of 18th AIAA/CEAS Aeroacoustics Conference (33rd AIAA Aeroacoustics Conference)*, No. AIAA 2012-2277, Colorado Springs, Colorado, 4-6 June 2012.

[27]Smith, M. J. T., *Aircraft noise*, Cambridge aerospace series, Cambridge University Press, 1989.